Bioorganic & Medicinal Chemistry Letters 23 (2013) 3051–3058

Contents lists available at SciVerse ScienceDirect

Bioorganic & Medicinal Chemistry Letters

journal homepage: www.elsevier.com/locate/bmcl

The design and synthesis of a potent glucagon receptor antagonist with favorable physicochemical and pharmacokinetic properties as a candidate for the treatment of type 2 diabetes mellitus

Angel Guzman-Perez *, Jeffrey A. Pfefferkorn, Esther C. Y. Lee, Benjamin D. Stevens, Gary E. Aspnes, Jianwei Bian, Mary T. Didiuk, Kevin J. Filipski, Dianna Moore, Christian Perreault, Matthew F. Sammons, Meihua Tu, Janice Brown, Karen Atkinson, John Litchfield, Beijing Tan, Brian Samas, William J. Zavadoski, Christopher T. Salatto, Judith Treadway

Pfizer Wordwide Research and Development, Eastern Point Road, Groton, CT 06442, USA

ARTICLE INFO

Article history:
Received 8 January 2013
Revised 26 February 2013
Accepted 4 March 2013
Available online 13 March 2013

Keywords:
Glucagon receptor antagonist
Diabetes mellitus
Physicochemical properties

ABSTRACT

A novel and potent small molecule glucagon receptor antagonist for the treatment of diabetes mellitus is reported. This candidate, (*S*)-3-[4-(1-{3,5-dimethyl-4-[4-(trifluoromethyl)-1*H*-pyrazol-1-yl]phenoxy}butyl)benzamido]propanoic acid, has lower molecular weight and lipophilicity than historical glucagon receptor antagonists, resulting in excellent selectivity in broad-panel screening, lower cytotoxicity, and excellent overall in vivo safety in early pre-clinical testing. Additionally, it displays low in vivo clearance and excellent oral bioavailability in both rats and dogs. In a rat glucagon challenge model, it was shown to reduce the glucagon-elicited glucose excursion in a dose-dependent manner and at a concentration consistent with its rat in vitro potency. Its properties make it an excellent candidate for further investigation.

Diabetes mellitus is a rapidly expanding public health problem affecting approximately 347 million people worldwide.[1] Type 2 diabetes mellitus is a metabolic disease in which fasting and postprandial plasma glucose is elevated due to abnormally high hepatic glucose production, reduced glucose-stimulated insulin secretion and insulin resistance.[2] Despite there being several classes of drugs in common clinical use, there is a significant need for new therapies with improved safety and efficacy, in order to help patients achieve appropriate glycemic control and avoid the long term complications associated with the disease.[3]

Glucagon is a polypeptide hormone produced and secreted by α-cells located in the endocrine portion of the pancreas. In the liver, glucagon binding to the glucagon receptor triggers a signal transduction cascade resulting in the stimulation of hepatic glucose production through glycogenolysis and gluconeogenesis. In type 2 diabetic patients, glucagon levels are inappropriately elevated in the fasted state and not adequately suppressed in the postprandial state, which contributes to the elevated hepatic glucose production and plasma glucose levels seen in these patients.[4] Consequently, it has been postulated that a reduction in glucagon action in the liver, brought about by a glucagon receptor antagonist, could reduce hepatic glucose production in type 2 diabetics, resulting in improved glycemic control. This hypothesis is supported by both preclinical and clinical data.[5]

The identification of clinically useful small molecule glucagon receptor antagonists for this class B G-protein coupled receptor has been very difficult. Recently, Merck reported the discovery of MK-0893 (**1**) as a clinical candidate, and several other related series also containing a β-alanine side chain such as compound **2**.[6] Lilly has also recently presented phase 1 data for LY2409021, a glucagon receptor antagonist of undisclosed structure.[7] Most of the reported glucagon receptor antagonists are lipophilic molecules with relatively high molecular weight as exemplified by **1** and **2** (Fig. 1).[8] In order to improve safety and biopharmaceutical properties, we focused our efforts on identifying a series of small molecule glucagon receptor antagonists with reduced lipophilicity ($\log D$ <3) and molecular weight (⩽500).[9]

Previously, we described the identification of a series of pyrazole ethers and amino pyrazoles, exemplified by compound **3**, with low molecular weight and $\log D$.[10] Unfortunately, despite their low dog plasma clearance, these compounds suffered from high rat plasma clearance which complicated rat toxicology studies and reduced the confidence in predictions of human pharmacokinetics. Further, it was discovered that some of the favored compounds from this series had undesired PPAR-δ agonist activity (for example, the PPAR-δ EC_{50} for **3** is 440 nM). Consequently, we explored

* Corresponding author at present address: Therapeutic Discovery, Amgen Inc., 360 Binney St., Cambridge, MA 02142, USA. Tel.: +1 617 444 5070.
E-mail address: aguzmanp@amgen.com (A. Guzman-Perez).

0960-894X/$ - see front matter © 2013 Elsevier Ltd. All rights reserved.
http://dx.doi.org/10.1016/j.bmcl.2013.03.014

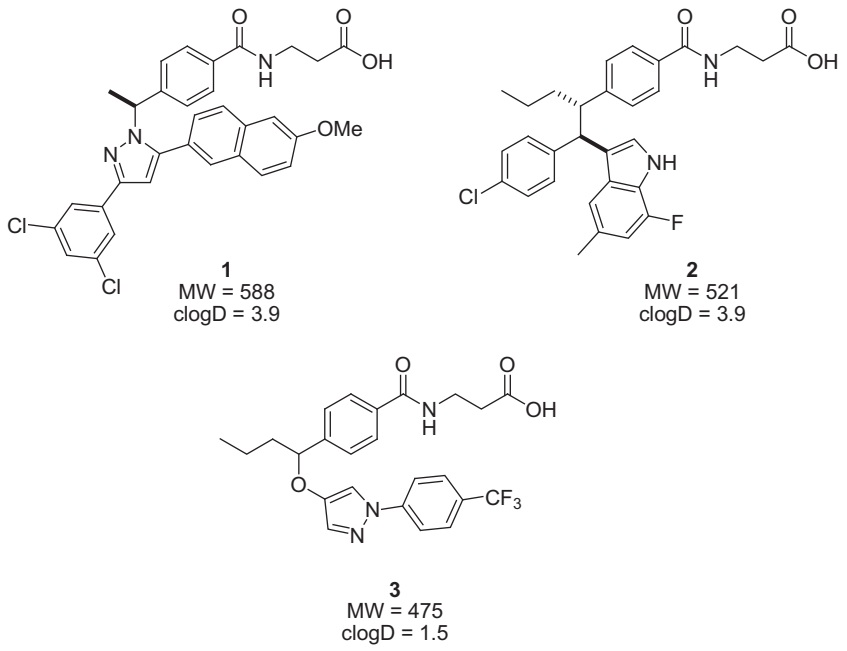

Figure 1. Structures of glucagon receptor antagonists **1**–**3**.

whether polarity could be transposed to the aromatic ring most distal from the acid. This led to the discovery of a new series of polar and low molecular weight glucagon receptor antagonists with improved properties.

The synthesis of the nitrogen-linked versions of these compounds was accomplished as exemplified in Scheme 1. Aniline **5** was prepared in two steps starting from 4-fluoronitrobenzene and 4-trifluoromethylpyrazole, which were coupled to afford intermediate **4**. The nitro functionality in **4** was reduced under transfer hydrogenation conditions to provide **5** in quantitative yield. Butyryl benzoate **6** was synthesized by reacting the Knochel-type Grignard reagent prepared from ethyl-4-iodobenzoate with butyraldehyde to afford the corresponding benzylic alcohol,[11] which was subsequently oxidized under Parikh–Doering conditions. Ketone **6** was an effective substrate for a reductive amination with *N*-heterocyclic aniline **5** using decaborane to afford ester **7**. It is worth noting that decaborane consistently proved superior to other reductive amination reagents for related transformations

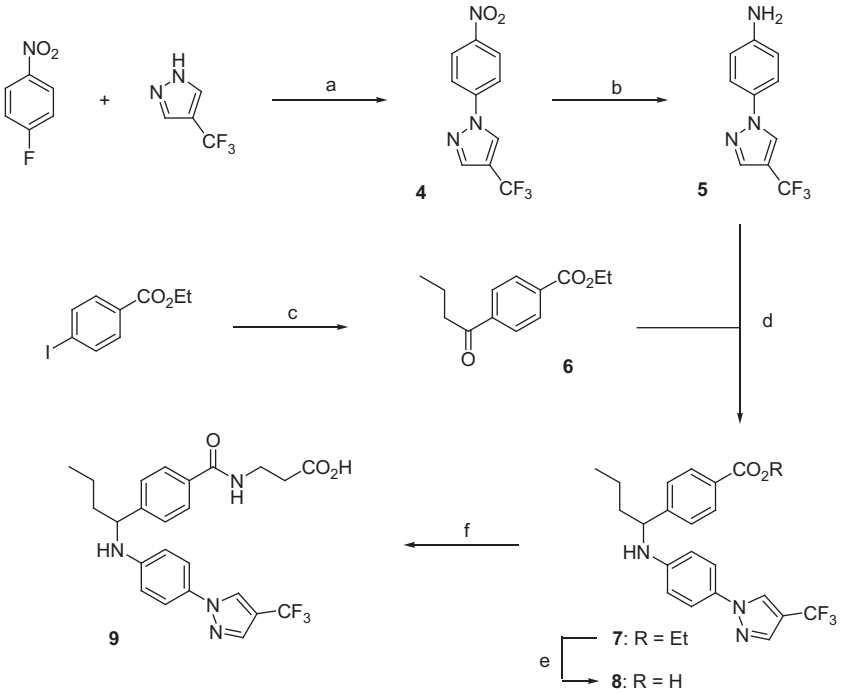

Scheme 1. Synthetic method for the synthesis of nitrogen-linked analogs. Reagents and conditions: (a) K_2CO_3, MeCN, 80 °C, 70%; (b) 10% Pd/C, EtOH, THF, $NH_4{\cdot}HCO_2$, quant.; (c) (i) *i*PrMgCl·LiCl, butyraldehyde, THF, −40 °C, (ii) TEA, $SO_3{\cdot}$Pyr., DMSO, CH_2Cl_2, 0 °C, quant.; (d) decaborane, MeOH, 0 °C; (e) 2:1 MeOH: 2.0 M aq LiOH, 66% for two steps; and (f) (i) ethyl-β-alanine·HCl, EDCI, DIPEA, HOBt, THF, (ii) 2:1 MeOH: 2.0 M aq LiOH, 56%.

within this target class.[12] Carboxylic acid **8** was prepared via base-mediated hydrolysis of **7**. A standard amide coupling with β-alanine ethyl ester, followed by subsequent ester hydrolysis gave the desired carboxylate **9**. The racemic mixture was resolved by chiral supercritical fluid chromatography to provide the separate enantiomers.

The corresponding ether linked compounds were synthesized as exemplified in Scheme 2. Ketone **6** was reduced to the corresponding (*R*)-alcohol **10** via transfer hydrogenation using an (*R*,*R*)-Noyori catalyst.[13] The 87% ee material from the Noyori hydrogenation was then enriched to >99% ee by chiral supercritical fluid chromatography. Hydrolysis of the ethyl ester to acid **11** enabled a standard amide coupling with β-alanine ethyl ester to obtain alcohol **12**. Separately, 4-bromo-2,6-dimethylaniline was transformed to the corresponding hydrazine hydrochloride **13** via diazotization and reduction with stannous chloride. The hydrazine was converted to pyrazole **14** by base-promoted cyclization with a β-trifluoromethyl vinamidinium salt, which was in turn synthesized by a Vilsmeier–Haack reaction of 3,3,3-trifluoropropanoic acid with phosphorus oxychloride in DMF at 70 °C followed by salt isolation with sodium hexafluorophosphate.[14] Aryl bromide **14** was then converted to phenol **15** via a palladium-catalyzed transformation using *t*BuXPhos.[15] A Mitsunobu reaction was then executed to join enantioenriched alcohol **12** and phenol **15** to deliver ether **16** in good yield. As expected, the reaction proceeded with complete inversion of the stereocenter (>99% ee). Subsequent ester hydrolysis provided the desired (−)-carboxylic acid **17**.[16] In other instances, racemic alcohols similar to **10** were used to provide racemic analogs, which in several cases were resolved by chiral supercritical fluid chromatography either at the final acid stage or at the penultimate ester. Additionally, several analogs were prepared by copper-catalyzed coupling (CuI/8-hydroxyquinoline) of an aryl iodide with the appropriate heterocycle to provide intermediates similar to **16**.[17]

The in vitro potency of test compounds was assessed using both binding and functional assay formats. The binding affinity of compounds for the human glucagon receptor was determined by their ability to displace [^{125}I] Glucagon-Cex from membranes containing the human glucagon receptor,[18] while functional activity was determined by the ability of these compounds to inhibit glucagon-induced cAMP production in a cell line expressing the human glucagon receptor. We were unable to perform these assays in the absence of serum to determine a free potency for the antagonists, because of the high degree of non-specific binding exhibited by glucagon. Consequently, the binding assay was performed in the presence of 0.2% bovine serum albumin (BSA), while functional activity was determined in the presence of 4% BSA in order to provide an estimate of the antagonists' plasma bound or total potency.

In addition to the molecular weight and polarity requirements outlined above, we also set forth the following objectives: (a) maintain a low in vivo clearance to obtain a moderate half-life despite the low volume of distribution typical of acids, (b) accordingly, target little to no turnover in microsomes, (c) maintain permeability and solubility as high as possible to facilitate absorption, which can be a challenge for high molecular weight acids, and (d) obtain a functional potency of <300 nM in the human cAMP assay in order to acquire an acceptable human dose prediction. For reference, compound **1** had a K_b of 270 nM in our human glucagon receptor (hGCGR) cAMP assay.

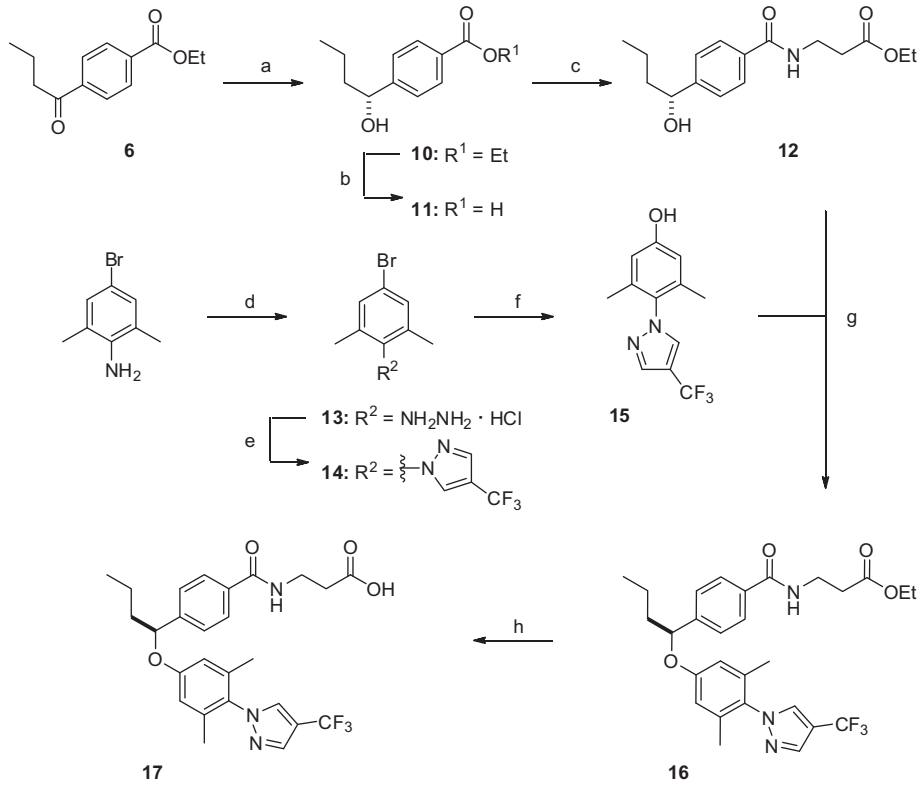

Scheme 2. Synthetic method for the synthesis of ethers. Reagents and conditions: (a) (i) [*N*-[(1*R*,2*R*)-2-(amino-κ*N*)-1,2-diphenylethyl]-4-methylbenzenesulfonamidato-κ*N*]chloro[(1,2,3,4,5,6-η)-1,3,5-trimethylbenzene]-ruthenium (2.5 mol %), 5:2 HCO_2H/Et_3N, 25 °C, 12 h, 99% yield, 86% ee, (ii) Chiralpak AD-H, SFC Mobile phase 80:20 CO_2/Methanol, 90% yield, 99% ee after resolution; (b) LiOH·H_2O, THF/H_2O/MeOH (1:1:1), 25 °C, 2.5 h, 93% yield, >99% ee; (c) β-alanine ethyl ester hydrochloride, HATU, DIPEA, DMF, 25 °C, 1 h, 95%, >99% ee; (d) (i) HCl (concd)/H_2O (1:2), 0 °C, 15 min then $NaNO_2$, H_2O, 0 °C, 30 min, (ii) $SnCl_2$·H_2O; HCl (concd)/H_2O (1:1), 0 °C, 1 h then 25 °C, 18 h, (iii) HCl/CH_3OH, EtOAc, 0 °C, 25 min, 64%; (e) (i) NaOMe, (*Z*)-*N*-(3-(dimethylamino)-2-(trifluoromethyl)allylidene)-*N*-methylmethanaminium hexafluorophosphate, 0–25 °C, 18 h, (ii) TFA, 80 °C, 5 h, 70%; (f) KOH, Pd_2dba_3, *t*BuXPhos, dioxane/H_2O (1:1), 95 °C, 1 h, 91%; (g) ADDP, Bu_3P, THF, 25 °C, 16 h, 75% yield, >99% ee; and (h) 1 N aq NaOH, MeOH/THF (1:1), 25 °C, 18 h, 87%, >99% ee.

The SAR of the nitrogen-linked analogs is summarized in Table 1. Incorporation of either a trifluoromethyl imidazole or trifluoromethyl pyrazole ring distal from the acid was tolerated as observed in compounds **18** and **19**. These compounds display modest potency in both the binding and functional assays, display good aqueous kinetic solubility at pH 6.5 (350–360 μM), and show no observable turnover in human (HLM) or rat liver microsomes (RLM). Importantly, as expected the incorporation of the heterocycles results in these compounds having log*D* values (shake-flask method using octanol/pH 7.4 buffer) in the range of interest. Both of these compounds were separated into single enantiomers and the most potent enantiomer of each was dosed intravenously to Wistar–Han rats at 1 mg/kg to determine their pharmacokinetic parameters. Unfortunately, the single enantiomers of compounds **18** and **19** had relatively high rat plasma clearances of 65 and 37 ml/min/kg, respectively.

Compounds **20**–**22** were prepared in an effort to eliminate the aniline motif from these molecules, and to optimize potency and reduce rat clearance. The trifluromethyl pyrazole group was chosen for this purpose due to the higher passive permeability (P_{app}) observed for **19** over **18** using the MDCKII-LE assay,[19] and its slightly enhanced potency. While pyridine analog **20** provided comparable potency and properties to **19**, pyridine **21** was clearly inferior. In contrast, pyrimidine analog **22** provided a moderate improvement in potency while reducing the log*D*. This compound also displays good kinetic solubility at pH 6.5 (380 μM) and no turnover in human or rat microsomes. The dimethyl analog **23** provided a significant improvement in binding potency over **19** that did not translate to the functional assay, and displayed moderate turnover in rat liver microsomes, thus it was not investigated further. Compounds **20** and **22** were separated into single enantiomers and the most potent enantiomer of each was used to determine their rat plasma clearance, which was 74 and 130 ml/min/kg, respectively. It is likely that the main clearance pathway of these compounds in rats is biliary excretion because: (a) there is no observable turnover in rat liver microsomes, (b) little to no drug was found in the urine of the rats, (c) efforts to detect glucuronidation in UGT-supplemented rat liver microsomes provided little to no turnover, (d) no plasma stability issues were detected, and (e) following a 5 mg/kg intravenous administration of the most potent enantiomer of **18**, 57% of the dose was collected in the bile. Interestingly, this may be rodent specific as the most potent enantiomer of **18** displays a plasma clearance of 2 ml/min/kg after a 0.5 mg/kg intravenous administration to Beagle dogs, and of 151 ml/min/kg after a 1 mg/kg intravenous administration to mice.

The corresponding ether linked compounds were also investigated and the results are summarized in Table 2. While the trifluoroimidazole ether (**24**) was significantly weaker than the corresponding aniline, the trifluoromethylpyrazole ether (**25**) was only twofold less potent than **19** in the functional assay. In addition, this compound possessed the desired polarity, acceptable passive permeability, no turnover in RLM, low turnover in HLM ($Cl_{int,app}$ 16 ml/min/kg) and good aqueous kinetic solubility at pH 6.5 (400 μM). Importantly, when **25** was separated into single enantiomers and the most potent enantiomer dosed to Wistar–Han rats at 1 mg/kg intravenously and 5 mg/kg orally, it provided a clearance from plasma of 17 ml/min/kg and an oral bioavailability of 60%. Given the favorable physicochemical, ADME and pharmacokinetic properties of ether **25**, we embarked on an effort to improve on its potency within the ether series. Replacement of the phenyl ring proximal to the pyrazole with a pyridine (**26**) or pyrimidine ring (**27**) did not provide the desired improvements in potency. This was particularly surprising in the pyrimidine case since this had improved potency in the N-linked series.

Modification of the alkyl side chain of **25** did not provide the required potency improvement (Table 3). Compounds **28**–**31** pro-

Table 1
In vitro properties of the nitrogen-linked analogs[a]

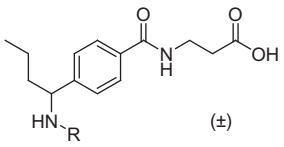

	R	Log*D*[b]	hGCGR binding K_i (nM)	hGCGR cAMP K_b (nM)	MDCKII-LE P_{app} ($\times 10^{-6}$ cm/s)
18	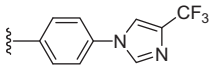	1.3	680	4700	0.6
19	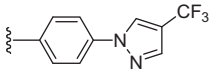	1.9	160[c]	2600	4.0
20	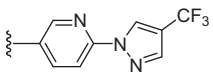	2.1	170	1300	4.6
21	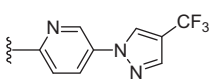	1.3	670	4100	0.8
22	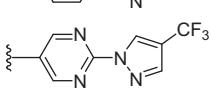	1.3	100	490	0.8
23	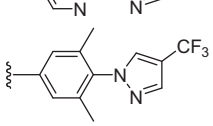	2.2	12	1400	2.7

[a] Binding and cAMP data is reported as the geometric mean of ⩾2 determinations except where otherwise noted.
[b] Log*D* values determined by shakeflask method.
[c] Value reported is $n = 1$.

Table 2
In vitro properties of ethers **24**–**27**[a]

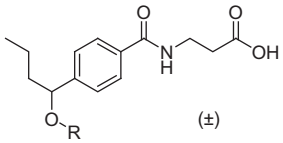

	R	Log*D*[b]	hGCGR binding K_i (nM)	hGCGR cAMP K_b (nM)	MDCKII-LE P_{app} ($\times 10^{-6}$ cm/s)
24	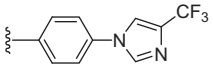	1.6	220	22000	2.3
25	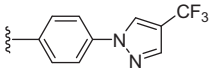	2.4	890	5100	3.1
26	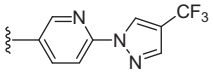	2.6	230	3700	3.4
27	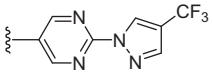	1.5[c]	1100		

[a] Binding and cAMP data is reported as the geometric mean of ⩾2 determinations except where otherwise noted.
[b] Log*D* values determined by shakeflask method.
[c] Estimated using an in silico model.

vided a slight improvement in potency but at the expense of unacceptable increases in lipophilicity, which were accompanied in most cases by an increase in microsomal turnover. Compounds **32**–**34** resulted in weaker potency than **25** in the functional assay. Interestingly, the ethyl analog **34**, the one carbon truncation of **25**, resulted in no activity in the cAMP assay.

Our efforts to optimize the trifluromethylpyrazole group are summarized in Table 4. Replacement of the trifluromethyl with a chloro substituent resulted in a compound (**35**) with similar potency and properties, with the exception of lower aqueous kinetic solubility at pH 6.5 (70 μM). Substitution with methyl or fluoro provided compounds (**36**–**37**) with lower lipophilicity but reduced potency in the cAMP assay. Remarkably, removal of the trifluoromethyl group as shown in compound **38** abolishes the functional activity. Attempts to utilize polar groups in place of the trifluoromethyl (**39**–**41**) also resulted in no functional activity. Addition of a methyl group at the 3-position (**42**) or fusion of a cyclohexyl ring to the pyrazole (**43**) provided similar potency with higher lipophilicity. Benzo fusion to the pyrazole afforded compound **44** with similar polarity and improved potency, but with moderate HLM turnover. This compound was separated into enantiomers and the most potent was dosed to Wistar–Han rats intravenously at 1 mg/kg and orally at 5 mg/kg. Unfortunately, although the compound's plasma clearance was 18 ml/min/kg, its oral bioavailability was only 3%. This is presumably the result of a combination of marginal passive permeability (P_{app} 2.2 $\times$ 10^{-6} cm/s) and low solubility, which was difficult to quantify.

Finally, we found (Table 5) that addition of two methyl groups *ortho* to the pyrazole ring resulted in a robust increase in potency in both the binding and functional assays (**45**). The (−)-(*S*)-enantiomer (**17**) was determined to be considerably more potent than (+)-(*R*)-enatiomer (**46**). Surprisingly, the enhancement in cAMP po-

Table 3
Alkyl side chain SAR of the ether series[a]

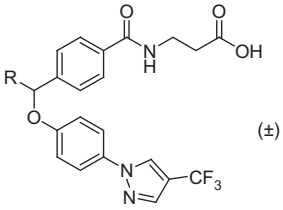

	R	Log*D*[b]	hGCGR binding K_i (nM)	hGCGR cAMP K_b (nM)	HLM $Cl_{int,app}$ (ml/min/kg)	RLM $Cl_{int,app}$ (ml/min/kg)
28	*cyclo*-Bu	2.6	700	3000	26	<25
29	*iso*-Bu	3.2	549	3400	23	46
30	*cyclo*-pentyl	3.3	420	4000	22	31
31	*tert*-Bu	3.7	170	4300	31	28
25	*n*-Pr	2.4	890	5100	16	<36
32	*iso*-Pr	2.6	720	8800	13	<25
33	*cyclo*-Pr	1.7	1300	15000	<8	<25
34	Et	1.9	1400	>22000	<8	<25

[a] Binding and cAMP data is reported as the geometric mean of ⩾2 determinations except where otherwise noted.
[b] Log*D* values determined by shakeflask method.

Table 4
Heterocyclic ring SAR of the ether series[a]

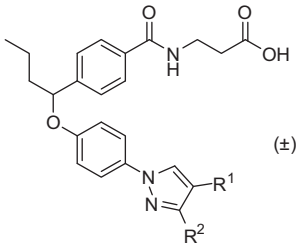

	R^1	R^2	Log D[b]	hGCGR binding K_i (nM)	hGCGR cAMP K_b (nM)	HLM $Cl_{int,app}$ (ml/min/kg)
25	CF_3	H	2.4	890	5100	16
35	Cl	H	2.6	1100	6500	10
36	Me	H	2.1	1900	11000	16
37	F	H	2.0	1700	10000	12
38	H	H	1.7[d]	4100[c]	>55000[c]	
39	CN	H	1.2	4100	>50000	<8
40	MeO	H	1.4	4400[c]	>23000[c]	<8
41	$C(O)NMe_2$	H	0.5	6500	>30000	<13
42	CF_3	Me	2.8	1100	8300	<10
43	$-CH_2-CH_2-CH_2-CH_2-$		2.7	690	4200	48
44	$-CH=CH-CH=CH-$		2.5	290	2000	44

[a] Binding and cAMP data is reported as the geometric mean of ⩾2 determinations except where otherwise noted.
[b] Log D values determined by shakeflask method.
[c] Value reported is $n = 1$.
[d] Estimated using an in silico model.

tency through addition of the two *ortho*-methyl groups was much larger in this series than the corresponding one observed in the N-linked series. It is also interesting to note that adding both methyl groups is important because compound **47** with only one *ortho*-methyl group afforded intermediate cAMP potency between **25** and **45**.

Compound **17** has excellent properties. Its log D is essentially the same as for **25** despite the presence of two additional methyl groups. This is likely due to a conformational effect where the pyrazole is forced to be almost perpendicular to the adjacent phenyl ring resulting in the *N*-2 of the pyrazole being more exposed to the solvent surface than in **25**. This additional polar surface area essentially cancels out the added lipophilicity from the two methyl groups. The absolute stereochemistry of **17** was confirmed to be (*S*) by X-ray crystallography and examination of the Hooft parameter.[20] Compound **17** has acceptable passive permeability (P_{app} 3.6×10^{-6} cm/s), no observable turnover in HLM or RLM, and good kinetic solubility at pH 6.5 (420 μM). In Caco-2 monolayers, it demonstrated a P_{app} of 8.5×10^{-6} cm/s at pH 7.4 and of 30×10^{-6} cm/s at pH 6.5. The enhanced permeability at lower pH is not surprising because the protonated form of the acid should have higher permeability, and is likely more relevant due to the acidic nature of the early gastrointestinal track. Its pharmacokinetic properties when dosed to rats and dogs are shown in Table 6. It has low clearance and high oral bioavailability in both species. The volume of distribution is low as expected and this results in short to moderate half-lives. The molecular weight for compound **17** is 503, which together with a log D of 2.6 (clog D 2.3) met our objectives. In contrast, compound **2** had an oral bioavailability of 7% and 30% after dosing at 5 mg/kg to rats and 4 mg/kg to dogs,

Table 5
Substitution at the phenyl ring of the ether series[a]

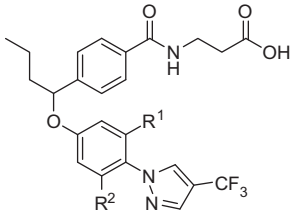

		R^1	R^2	Log D[b]	hGCGR binding K_i (nM)	hGCGR cAMP K_b (nM)
25	Racemic	H	H	2.4	890	5100
45	Racemic	Me	Me	2.6[c]	64	770
17	(−)-(*S*)	Me	Me	2.5	14	270
46	(+)-(*R*)	Me	Me	2.7	1600	9000
47	Racemic	Me	H	2.6	200	1900

[a] Binding and cAMP data is reported as the geometric mean of ⩾4 determinations except where otherwise noted.
[b] Log D values determined by shakeflask method.
[c] Estimated using an in silico model.

Table 6
Compound **17** pharmacokinetic properties[a]

Species	Plasma clearance (ml/min/kg)	Volume of distribution at steady state (L/kg)	Beta half-life (h)	Oral bioavailability (%)
Rat	2.8	0.40	1.8	100
Dog	1.5	0.31	2.5	100

[a] Wistar–Han rats dosed at 1 mg/kg intravenously and 50 mg/kg orally. Beagle dogs dosed at 0.5 mg/kg intravenously and 5 mg/kg orally.

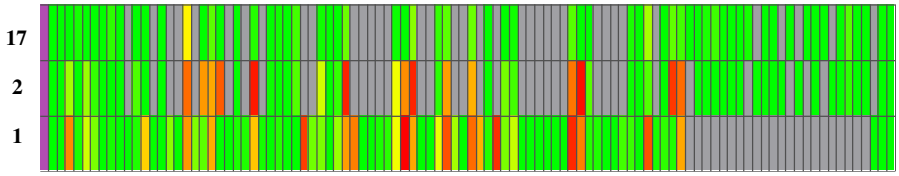

Figure 2. Heat map of the activity of compounds **17**, **1** and **2** against a panel of pharmacological targets at 10 μM. Each column is a separate assay. Color gradient with green = 0% effect, yellow = 50% effect and red = 100% effect.

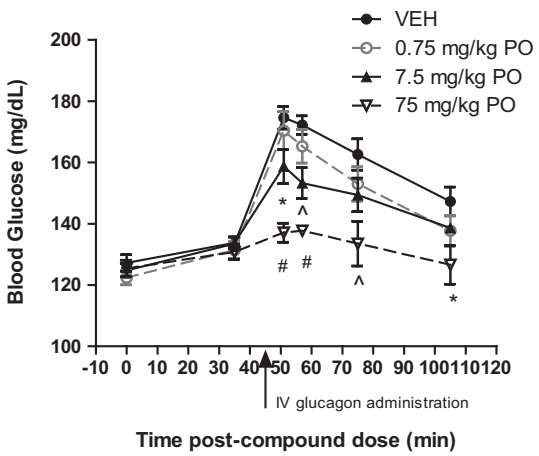

Figure 3. Effects of **17** dosed orally in the rat glucagon challenge model ($N = 6$, $^{*}p < 0.05$, $^{\wedge}p < 0.01$, $^{\#}p < 0.001$).

respectively. The low bioavailability may be, at least partially, due to the low kinetic solubility of compound **2** at pH 6.5 (23 μM).

Compound **17** has also excellent selectivity against a panel of 69 receptors, ion channels, uptake sites and enzymes tested at 10 μM, with >50% activity only identified for the rat chloride (GABA-gated) channel ($K_i = 8.2$ μM). This is in contrast with the numerous hits identified when compounds **1** and **2** were screened at the same concentration in similar panels. A comparison is best visualized in the heat map in Figure 2. Compound **17** also displayed no agonist activity at 10 μM when tested in PPAR-α, δ, and γ assays. It has a binding K_i of 3160 nM for the GLP-1 receptor which provides 230-fold selectivity when compared to the glucagon binding K_i. Selected compounds were also assessed in a transformed human liver epithelial (THLE) cell cytotoxicity assay. This assay measures ATP depletion as a determinant of general cellular toxicity at 72 h, and has been found to correlate with pre-clinical in vivo toxicity.[21] Compound **17** had an IC_{50} of 112 μM, suggestive of lower toxicity than reference compounds **1** ($IC_{50} = 38$ μM) and **2** ($IC_{50} = 55$ μM). Furthermore, compound **17** displayed an excellent safety profile in 14-day exploratory toxicological studies in rats and dogs. Together this data suggests that compound **17** may offer a reduced safety risk profile than that of more lipophilic glucagon receptor antagonists.

Compound **17**, like most compounds investigated in this series, showed weaker potency in the rat, mouse and dog glucagon receptor functional assays than in the corresponding human assay. Compound **17** afforded in the rat cAMP assay a K_b of 3900 nM, in the mouse cAMP assay a K_b of 1500 nM, in the dog assay a K_b of 1200 nM, and in the monkey cAMP assay a K_b of 82 nM. As a result of the excellent rat pharmacokinetic properties of **17** and despite its weak rat potency, it was possible to assess it in an in vivo rat glucagon challenge model. In this study, Wistar–Han rats ($n = 6$) were administered either **17** or vehicle orally followed 45 min later by a 3 μg/kg intravenous challenge of glucagon. At predetermined timepoints pre- and post-glucagon administration, plasma samples were collected for the assessment of glucose and plasma levels of **17**. As shown in Figure 3, **17** suppressed the glucagon induced glucose excursion in a dose proportional manner, with the 75 mg/kg dose almost completely blocking the glucose elevation. The 7.5 mg/kg dose provides approximately 50% reduction in the glucose excursion. The bound plasma exposure during the experiment of **17** at a dose of 7.5 mg/kg was consistent in magnitude with the compound's in vitro rat K_b, demonstrating good rat in vitro–in vivo translation. The results from this model not only confirm the in vivo activity of **17**, but also support our use of the in vitro cAMP assay at 4% BSA as a good predictor of in vivo potency.

In summary, we have identified compound **17** as a potent glucagon receptor antagonist for the treatment of diabetes mellitus. This compound has lower molecular weight and lipophilicity than historical glucagon receptor antagonists, which results in excellent selectivity in broad-panel screening, lower cytotoxicity, and excellent overall in vivo safety in early pre-clinical testing. This compound displays low in vivo clearance and excellent oral bioavailability in both rats and dogs. In a rat glucagon challenge model, compound **17** was shown to reduce the glucagon-elicited glucose excursion in a dose-dependent manner and at a concentration consistent with its rat in vitro potency. Taken together the overall properties of **17** supported its selection as an early development candidate for the treatment of type 2 diabetes mellitus.

Acknowledgements

The authors would like to acknowledge Mei Li and David A. Perry at Pfizer for strategic outsourcing. Additionally, we thank Hong Li and the team at BioDuro in Beijing, China for their technical assistance running the glucagon challenge, and Jinfei Li, Zhanshan Qian and the team at WuXi AppTec in Shanghai, China for synthetic assistance. Finally, we thank Manthena Varma and Charles Rotter for performing the Caco-2 permeability determinations.

References and notes

1. Danaei, G.; Finucane, M. M.; Lu, Y.; Singh, G. M.; Cowan, M. J.; Paciorek, C. J.; Lin, J. K.; Farzadfar, F.; Khang, Y.-H.; Stevens, G. A.; Rao, M.; Ali, M. K.; Riley, L. M.; Robinson, C. A.; Ezzati, M. *Lancet* **2011**, *378*, 31.
2. Saltiel, A. R. *Cell* **2001**, *104*, 517.
3. Krentz, A. J.; Patel, M. B.; Bailey, C. J. *Drugs* **2008**, *68*, 2131.
4. Dunning, B. E.; Gerich, J. E. *Endocr. Rev.* **2007**, *28*, 253.
5. (a) Ali, S.; Drucker, D. J. *Am. J. Physiol. Endocrinol. Metab.* **2009**, *296*, E415; (b) Engel, S. S.; Xu, L.; Andryuk, P. J.; Davies, M. J.; Amatruda, J.; Kaufman, K.; Goldstein, B. J. *Diabetes* **2011**, *60*, A85.
6. (a) Parmee, E. R. Abstracts of Papers, *241st National Meeting of the American Chemical Society*, Anaheim, CA; American Chemical Society: Washington, DC, 2011; Abstract MEDI-31.; (b) Xiong, Y.; Guo, J.; Candelore, M. R.; Liang, R.; Miller, C.; Dallas-Yang, Q.; Jiang, G.; McCann, P. E.; Qureshi, S. A.; Tong, X.; Xu, S. S.; Shang, J.; Vincent, S. H.; Tota, L. M.; Wright, M. J.; Yang, X.; Zhang, B. B.; Tata, J. R.; Parmee, E. R. *J. Med. Chem.* **2012**, *55*, 6137; (c) Shen, D.-M.; Lin, S.; Parmee, E. R. *Exp. Opin. Ther. Patents* **2011**, *21*, 1211.
7. Kelly, R. P.; Garhyan, P.; Abu-Raddad, E. J.; Fu, H.; Lim, C. N.; Prince, M. J.; Pinaire, J. A.; Loh, M. T.; Deeg, M. A. *Diabetes* **2011**, *60*, A84.
8. DeMong, D. E.; Miller, M. W.; Lachowicz, J. E. *Annu. Rep. Med. Chem.* **2008**, *43*, 119.
9. (a) Edwards, M. P.; Price, D. A. *Annu. Rep. Med. Chem.* **2010**, *45*, 381; (b) Leeson, P. D.; Empfield, J. R. *Annu. Rep. Med. Chem.* **2010**, *45*, 393; (c) Hughes, J. D.; Blagg, J.; Price, D. A.; Bailey, S.; DeCrescenzo, G. A.; Devraj, R. V.; Ellsworth, E.; Fobian, Y. M.; Gibbs, M. E.; Gilles, R. W.; Greene, N.; Huang, E.; Krieger-Burke, T.; Loesel, J.; Wagner, T.; Whiteley, L.; Zhang, Y. *Bioorg. Med. Chem. Lett.* **2008**, *18*, 4872; (d) Price, D. A.; Blagg, J.; Jones, L.; Greene, N.; Wager, T. *Exp. Opin. Drug Metab. Toxicol.* **2009**, *5*, 921.
10. Filipski, K. J.; Bian, J.; Ebner, D. C.; Lee, E. C. Y.; Li, J.-C.; Sammons, M. F.; Wright, S. W.; Stevens, B. D.; Didiuk, M. T.; Tu, M.; Perreault, C.; Brown, J.; Atkinson, K.; Tan, B.; Litchfield, J.; Pfefferkorn, J. A.; Guzman-Perez, A. *Bioorg. Med. Chem. Lett.* **2012**, *22*, 415.
11. Ren, H.; Krasovskiy, A.; Knochel, P. *Org. Lett.* **2004**, *6*, 4215.
12. Bae, J. W.; Lee, S. H.; Cho, Y. J.; Yoon, C. M. *J. Chem. Soc., Perkin Trans. 1* **2000**, 145.
13. Fujii, A.; Hashiguchi, S.; Uematsu, N.; Ikariya, T.; Noyori, R. *J. Am. Chem. Soc.* **1996**, *118*, 2522.
14. (a) Yamanaka, H.; Takekawa, T.; Morita, K.; Ishihara, T. *Tetrahedron Lett.* **1829**, *1996*, 37; (b) Davies, I. W.; Marcoux, J.-F.; Wu, J.; Palucki, M.; Corley, E. G.; Robbins, M. A.; Tsou, N.; Ball, R. G.; Dormer, P.; Larson, R. D.; Reider, P. J. *J. Org. Chem.* **2000**, *65*, 4571.
15. Anderson, K. W.; Ikawa, T.; Tundel, R. E.; Buchwald, S. L. *J. Am. Chem. Soc.* **2006**, *128*, 10694.
16. Compound **17**: ^{1}H NMR (400 MHz, $CDCl_3$) δ: 7.88 (s, 1H), 7.73 (d, J = 8.2 Hz, 2H), 7.65 (s, 1H), 7.39 (d, J = 8.4 Hz, 2H), 6.80 (t, J = 5.9 Hz, 1H), 6.56 (s, 2H), 5.16 (dd, J = 7.8, 5.1 Hz, 1H), 3.71 (q, J = 5.9 Hz, 2H), 2.69 (t, J = 5.8 Hz, 2H), 2.04–1.91 (m, 1H), 1.88 (s, 6H), 1.86–1.67 (m, 1H), 1.63–1.31 (m, 2H), 0.96 (t, J = 7.3 Hz, 3H). MS (M+1): 504. Mp: 157–159 °C. $[\alpha]_D = -43.8$ (c = 1; $CHCl_3$). Chiral SFC. Column: Chiralpak AD-H. Dimensions: 10 × 250 mm. Mobile phase: 80/20 CO_2/2-propanol. Flow rate: 10.0 mL/min. Modifier: 0.2% isopropylamine. Retention time: 3.23 min (first peak).
17. Filipski, K. J.; Kohrt, J. T.; Casimiro-Garcia, A.; Van Huis, C. A.; Dudley, D. A.; Cody, W. L.; Bigge, C. F.; Desiraju, S.; Sun, S.; Maiti, S. N.; Jaber, M. R.; Edmunds, J. J. *Tetrahedron Lett.* **2006**, *47*, 7677.
18. Li, P.; Rogers, R.; Smiley, D.; DiMarchi, R. D.; Zhang, F. *Acta Crystallogr., Sect. F: Struct. Biol. Cryst. Commun.* **2007**, *63*, 599.
19. Di, L.; Whitney-Pickett, C.; Umland, J. P.; Zhang, H.; Zhang, X.; Gebhard, D. F.; Lai, Y.; Federico, J. J., III; Davidson, R. E.; Smith, R.; Reyner, E. L.; Lee, C.; Feng, B.; Rotter, C.; Varma, M. V.; Kempshall, S.; Fenner, K.; El-Kattan, A. F.; Liston, T. E.; Troutman, M. D. *J. Pharm. Sci.* **2011**, *100*, 4974.
20. (a) Hooft, R. W. W.; Straver, L. H.; Spek, A. L. *J. Appl. Crystallogr.* **2008**, *41*, 96; (b) Spek, A. L. *J. Appl. Crystallogr.* **2003**, *36*, 7.
21. Greene, N.; Aleo, M. D.; Louise-May, S.; Price, D. A.; Will, Y. *Bioorg. Med. Chem. Lett.* **2010**, *20*, 5308.